IEEE Access
Multidisciplinary ⋮ Rapid Review ⋮ Open Access Journal

Received 9 January 2024, accepted 22 January 2024, date of publication 31 January 2024, date of current version 7 March 2024.

Digital Object Identifier 10.1109/ACCESS.2024.3360852

RESEARCH ARTICLE

Self-Powered Cattle Behavior Monitoring System Using 915 MHz Radio Frequency Energy Harvesting

THAI HA DANG[1], LIONEL NKENYEREYE[2], VIET-THANG TRAN[3], AND WAN-YOUNG CHUNG[1], (Senior Member, IEEE)

[1]Department of Artificial Intelligence Convergence, Pukyong National University, Busan 48513, South Korea
[2]AI Convergence Education and Research Group, Busan 48513, South Korea
[3]Vietnam Research Institute of Electronics, Informatics and Automation, Ho Chi Minh City 70000, Vietnam

Corresponding author: Wan-Young Chung (wychung@pukyong.ac.kr)

The support for this study was provided by the National Research Foundation of Korea (NRF) through a grant from the Ministry of Science and ICT (MSIT) (No. 2019K1A3AIA05088484 and No.2019R1A2C1089139).

This work involved human subjects or animals in its research. Approval of all ethical and experimental procedures and protocols was granted by the Department of Livestock and Veterinary under Application No. ST251122VN.

ABSTRACT The accurate monitoring and management of dairy cattle behavior are critical for improving farm productivity as well as animal welfare and health status. In this paper, we present a self-powered dairy-cattle-behavior monitoring system that harnesses 915 MHz radio-frequency (RF) energy harvesting and bidirectional long short-term memory (Bi-LSTM) networks. The system aims to enable continuous and real-time monitoring of cattle behaviors while eliminating the need for battery replacements. By harvesting RF energy from the surrounding electromagnetic radiation, our system achieves long-term, self-sustainable operation, reducing maintenance efforts and costs. The Bi-LSTM network effectively captures the temporal dependencies and patterns in the collected sensor data, enabling accurate behavior recognition and prediction. Experimental results demonstrate the effectiveness of the proposed system in accurately classifying cattle behaviors, with an overall accuracy of 96.79%. Compared with traditional manual observation methods and battery-dependent systems, our self-powered monitoring system offers enhanced automation, improved welfare monitoring, and increased operational efficiency. The combination of RF energy harvesting, and Bi-LSTM networks affords a promising approach for self-powered and intelligent dairy-cattle-behavior monitoring, facilitating optimized management practices in the dairy industry.

INDEX TERMS Cattle monitoring system, radio-frequency energy harvesting, bi-directional long short-term memory, one-dimensional convolutional neural network deep learning.

I. INTRODUCTION

The monitoring and management of dairy cow behavior plays a crucial role in modern dairy farming. By understanding the behavioral patterns of cattle, farmers can detect health issues, optimize feeding strategies, and improve overall herd management [1]. Traditional manual observation methods are time-consuming and labor-intensive, and they may not enable continuous monitoring [2]. Therefore, there is a growing demand for automated and accurate systems that can continuously monitor and analyze dairy cow behavior.

The physical behavior of dairy cattle indicates their well-being, health status, and productivity [3]. Abnormal behaviors, such as reduced feed intake, prolonged lying time, and decreased locomotion, can be early signs of diseases, discomfort, or environmental stress [4]. Timely detection and intervention can lead to improved cow welfare, increased milk production, and reduced veterinary costs [5]. Therefore,

The associate editor coordinating the review of this manuscript and approving it for publication was Mohamed Kheir.

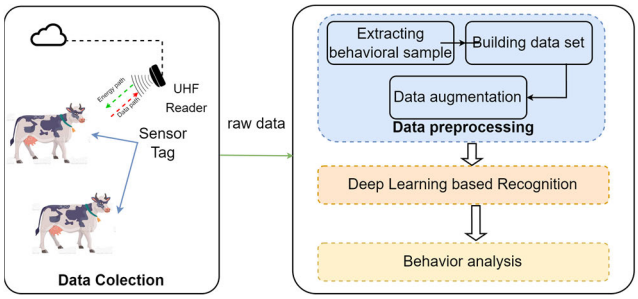

FIGURE 1. The proposed conceptual model of the dairy cow monitoring system powered by 915 MHz Energy Harvesting.

an automated monitoring system that can accurately recognize and classify cow behaviors in real time is of great significance to dairy farmers.

Energy-harvesting techniques have emerged as a promising solution for powering wireless sensor networks, enabling long-term and self-sustainable operation without requiring battery replacement [6]. Radio-frequency (RF) energy harvesting, in particular, has gained attention because of its ability to extract energy from ambient electromagnetic radiation [7]. By harnessing RF energy, we can develop a self-powered monitoring system that eliminates the need for frequent battery replacements, reducing maintenance cost.

Wireless power transfer (WPT) techniques using RF energy harvesting can be classified into two types: near-field and far-field. Near-field WPT, the first type, employs inductive and magnetic resonance coupling [8]. Both inductive coupling and magnetic resonance coupling involve energy exchange between two coils, relying on magnetic coupling technology. While near-field WPT can achieve high power conversion efficiencies (PCE) of up to 80%, its effectiveness is constrained by the limited separation distance between the coils or resonators. The power attenuates rapidly with distance, with an attenuation rate of 60 dB per decade. This implies that the power diminishes by a factor of 106 for every 10-fold increase in distance.

The limitations of near-field WPT can be solved with the help of far-field WPT [9]. It uses radiative coupling, transferring energy via a wave-propagating electric field. The transmitter and receiver can deliver electricity over a significant distance of many meters using this technique. However, as the Friis equation [10] predicts, it likewise experiences a power attenuation rate of 20 dB per decade of travel. Far-field WPT is a good choice for remotely powering and charging sensor devices despite this attenuation. The current study concentrates on RF energy harvesting, especially far-field WPTs, using this advantage.

In order to create an effective RF energy harvester, several crucial aspects need to be taken into account. Among related factors, the efficiency of the receiving antenna, the energy conversion efficiency, the sensitivity to the received energy and the operating modes can be optimized to increase the energy efficiency of the device [11]. Properly modeling the circuitry, a vital element in the design process, is one of the difficulties in creating such harvesters. A low-input RF signal is frequently extracted into a useful voltage using charge pumps. At high frequencies, they do, however, behave in a highly nonlinear manner that includes unanticipated capacitive and resistive effects. The energy-storage element, often a low-leakage capacitor, exhibits unpredictable fluctuations due to these factors, making it the most challenging part of an energy harvester to model.

Based on extensive research on the automatic monitoring of cow behaviors, there are two types of cow behavior monitoring techniques: contact-based and non-contact-based [12]. Cameras are deployed in farms as part of the non-contact strategy to observe and document cow behavior. Although the cattle are at ease using this method because there are no devices linked to them, it has a restricted deployment window, especially for grazing animals. In contrast, the sensor-based contact method entails fastening several sensor kinds to the cattle in order to collect data on their body temperatures, breathing rates, and motion velocities [13]. In earlier investigations, researchers measured pressure using a noseband pressure sensor installed on a cow's nose bridge.

The utilization of commercial, low-cost acceleration sensors is a promising strategy for monitoring dairy cow behavior. Due to their small size and lightweight attribute, they exert minimal impact on cow comfort, making them suitable for application in behavioral recognition systems. Accelerometers have proven to be reliable for detecting and classifying various cow behaviors, making them an essential component of behavior recognition systems [14]. This study focused on classifying dairy cow activities using data from a sensor tag, a collar-mounted device with an integrated accelerometer.

Numerous monitoring systems have been developed for observing dairy cow behavior, many of which incorporate embedded sensors [15]. While these systems are generally reliable and deliver precise classification outcomes, there are still various design considerations to address, particularly regarding the power source's lifespan for wearable devices. Wearable gadgets rely on batteries to supply the necessary electricity for their internal circuitry. Although the battery life of these devices can last for several years, opting for a larger battery capacity, assuming a constant voltage level, extends the device's operational duration but also leads to increased size, weight, and manufacturing costs [16]. Moreover, batteries require periodic replacement (for non-rechargeable batteries) or recharging (for rechargeable batteries), resulting in the increasing operational expenses and potential disruptions in continuous monitoring [17]. In the worst case, battery damage can lead to the leakage of harmful chemicals, adversely impacting the well-being of dairy animals. As a result, researchers have directed their attention towards energy-harvesting technologies as a solution for replenishing batteries in dairy-cow monitoring systems.

In order to showcase the practicality of the proposed system, we developed an RF energy harvesting module integrated with a sensor circuit. This module enabled the tag to

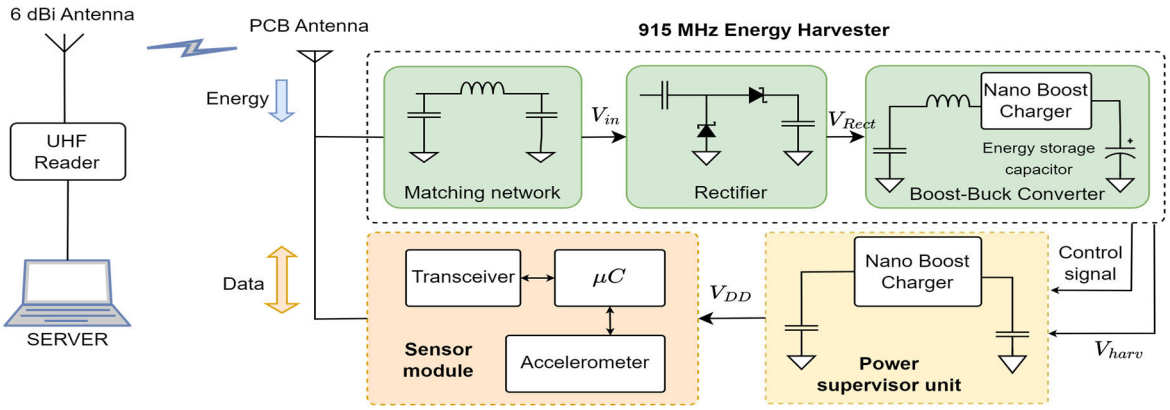

FIGURE 2. The block design of the proposed battery less collar-mounted sensor tag.

harness power from a specific RF transmitter. Through experiments, we evaluated the wearable device's ability to capture energy and its overall usability. Subsequently, we conducted a two-week demonstration on a dairy farm, utilizing the proposed system to identify and categorize various actions in dairy cattle. For this purpose, we created bidirectional long short-term memory (Bi-LSTM) and one-dimensional convolutional neural network (1D-CNN) deep learning models for behavior classification.

Furthermore, we conducted a comparison between the proposed model and traditional machine learning approaches such as the multilayer perceptron (MLP) [18] and the support vector machine (SVM) [19]. Unlike previous studies that predominantly focused on using feature computation and classification models to address classification tasks, our research introduces a novel approach that employs the data collected from the sensor tag as input for deep learning classification models. Leveraging the Bi-LSTM model, we effectively analyze time series data, while CNN excels in image processing and time-varying signal analysis. One notable advantage of these models is their ability to directly process raw data, eliminating the need for complex feature calculations at the input stage.

The following is the organization of the remaining sections of this paper. The proposed battery-free cow monitoring system is fully described in Section II. The energy harvesting performance of the sensor tag is also evaluated. The architecture of the neural network classification models under investigation and an overview of the tests carried out on a dairy farm are all introduced in Section III. Section IV compares the performance and classifiably of the proposed Bi-LSTM model with three different machine learning classifiers. Additionally, the section presents the results obtained from monitoring four specific dairy cow behaviors. Finally, Section V concludes the study.

II. PROPOSED SYSTEM

A power harvester capable of extracting energy at low-power densities was meticulously developed to facilitate the self-powered functionality of the cow-behavior monitoring system. The energy harvester module architecture is depicted in Fig. 2, and it comprises a PCB antenna, an energy-harvesting circuit, a supercapacitor for energy storage, and a sensor module for data collection and sensing.

A. PCB-PRINTED ANTENNA DESIGN

The antenna constitutes the primary element and assumes a pivotal role in the RF energy-harvesting system [20]. It functions as the intermediary between the ambient electromagnetic radiation and the energy-harvesting circuitry, thereby facilitating effective energy conversion and storage. The antenna's design plays a critical role in ensuring high efficiency, especially considering the relatively low density of RF energy in open space [21]. In obstructed environments, isotropic antennas disperse energy uniformly in all directions, leading to an energy density that diminishes inversely with the square of the distance from the RF wave generator at each location. In the far-field region of free space, the amount of radiated energy that the receiver antenna can harvest is determined using Friis's equation as follows:

$$P_R = P_T \frac{G_T G_R \lambda^2}{(4\pi D)^2 L_P} \tag{1}$$

where P_T and P_R denote transmitted power from the transmitting antenna and the received power at the receiving antenna and the; G_T and G_R denote the gains of transmitting antenna and the receiving, respectively; D represents the distance between the transmitter and receiver; and the λ represents the wavelength of the signal.

In the context of an RF energy harvesting system with a dedicated source, specific predetermined parameters of the transmission antenna, including the gain, frequency, and transmit power, are carefully determined. Integrating a comparatively high-gain antenna within the harvested module enhances the power-collection capabilities. To fulfill these requirements, a modified, printed meander line antenna was developed in the present study. Meander line antennas are inherently compact because of their folded structure [22].

TABLE 1. The optimizes dimension of the proposed meander line antenna.

Symbol	Dimensions	Symbol	Dimensions
D_{sub}	45.5	D_{ground}	7
L_{sub}	55.5	L_{ground}	15
L_{feed}	30.41	W_{Trans}	0.6
W_{feed}	3.2	d_{line}	0.3
D_{trans}	0.7	W_{feed}	13.2

They can be designed to occupy small areas, making them suitable for integration into compact devices and systems. Furthermore, they can exhibit directional radiation patterns, focusing the captured energy in specific directions. This characteristic is beneficial for targeting and capturing energy from specific RF sources or maximizing the harvesting efficiency in a particular direction. Fig. 1 illustrates the design of the proposed PCB-printed antenna, while these optimized dimensions are shown in table 1.

The primary objective of the antenna design is to achieve impedance matching with the 50 Ω system impedance at the designated operating frequency. The minimization of the magnitude of return loss is of significance in the pursuit of efficient energy harvesting, as it directly corresponds to reduced power reflection relative to the incident power. In this study, a target return loss of −40 dB is sought-after. To optimize the dimensions of the antenna and fulfill the desired objectives, parametric analyses were performed. The aim was to establish a 50 Ω transmission line connecting the feed point of the antenna with the matching network. This was achieved by employing a coplanar waveguide technique. A substrate material with a thickness of 1.7 mm and a dielectric constant of 4.31 was carefully selected for the antenna design.

Fig. 4 (a) presents the return loss of the antenna, both from simulations and measurements. At the designated operating frequency of 915 MHz, the measured return loss is −37 dBm, which is consistent with the simulated value of −40 dBm. The antenna exhibits omnidirectional radiation patterns, as depicted in Fig. 4 (b), which indicates a favorable characteristic of low directivity. This omnidirectional behavior is highly desirable in RF energy-harvesting scenarios where the direction of the incident signal is unknown. The antenna achieves a peak gain of 1.79 dBi. Further elaboration on the antenna's harvested power performance is provided in the subsequent section. Comparing the reflection coefficients (S11) and VSWR acquired from the Ansys HFSS with those obtained from the CST MWS simulator allows us to confirm the accuracy of the simulation findings. To assess the antenna's performance, measurements were carried out in an anechoic chamber.

B. RADIO-FREQUENC Y ENERGY HARVESTER DESIGN

1) MATCHING NETWORK

The impedance-matching network plays a critical role in wireless power-transfer systems by enhancing the power

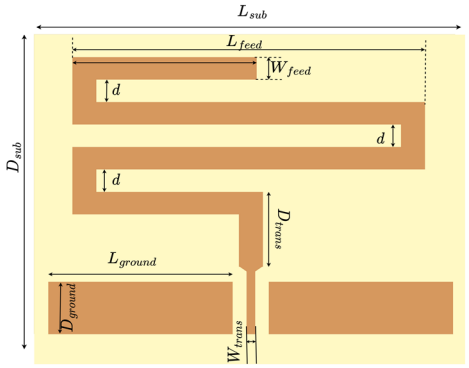

FIGURE 3. The geometry of a proposed printed meander line antenna.

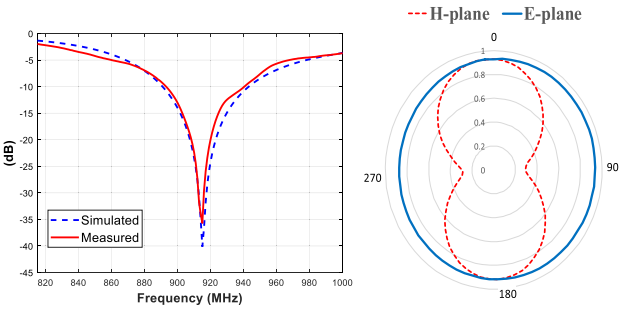

FIGURE 4. The proposed meandered line antenna performance: (a) return loss, (b) radiation patterns.

transfer efficiency from the antenna to the rectifier circuit and boosting the RF input voltage [23]. While DC circuits require identical resistances for optimum power transfer, RF circuits utilize impedance due to the reactance of inductor and capacitor. When the source and load impedances mismatch, a portion of the incident power is reflected to the source, which reduces the system's efficiency. For the receiving antenna and rectifier to transfer power as efficiently as possible, an impedance-matching network is required. There are many types of impedance-matching networks; however, in this design, the Pi matching network is chosen because it allows flexibility in the selection of inductors and capacitors and reduces power loss due to signal reflections.

2) VOLTAGE RECTIFIER

When designing energy harvesting circuits, it is important to ensure efficient operation at low RF power levels for optimal performance [24]. Among the main components in the energy collector, the rectifier is crucial in determining the efficiency of the circuit by regulating the output voltage. For far-field energy extraction applications, Dickson charge pumps are often preferred [25]. The selection of diodes and the determination of the number of stages are key factors in rectifier designs. Conventional diodes typically have a threshold voltage much higher than the maximum value generated by RF signal, so diodes with ultra-low voltage should be used. Therefore, for this study, Schottky diodes (SMS-7630, Sky-

works Technologies) with 150 mV on voltage were selected. It's critical that the diodes have quick switching capabilities rather than slower switching like regular diodes because the harvester circuit operates at extremely high frequencies.

The number of stages incorporated in a rectifier represents an important parameter that affects both the efficiency and the output voltage of the energy harvester [26]. While increasing the number of stages usually results in a proportional increase in the output voltage, achieving higher efficiency is not always guaranteed due to practical limitations such as power input RF and load impedance. In addition, incorporating additional stages often leads to increased power loss and performance degradation. Therefore, this study applies a single-stage Dickson-type configuration to the rectifier, creating a balance between output voltage and efficiency while minimizing power loss.

3) BOOST CONVERTER AND SUPERCAPACITOR SELECTION

To guarantee the continuous operation of the sensor module, it is essential to meet its minimum energy demand [27]. The disruption of the sensor module's operation due to energy shortage is an undesired scenario. To serve as the power source for the sensor module and store harvested energy, a supercapacitor (S_{CAP}) was used in this study. A BQ25570 nano boost converter with remarkable properties was used to enable effective supercapacitor charging. With an ultralow input power under 15 mW, this boost converter can start operating from input voltages as low as 100 mV and achieve peak voltages of 2.2–5 V. Thanks to the boost charger's built-in maximum power point tracking (MPPT) functionality, the harvester circuit can maximize the received energy from the radiated power source. The supercapacitor is charged and discharged within the allowable voltage limits thanks to the boost charger. The output voltage is regulated between 3.3 V - V_{HTHR} and 1.8 V -V_{LTHR}, to align with the operating voltage characteristics of the sensor module.

The selection of appropriate supercapacitor is crucial for the energy-storage component in our self-powered cow-behavior monitoring system [28]. Supercapacitors offer high energy density, fast charging and discharging capabilities, and long cycle life, making them suitable for capturing and storing the energy harvested from RF sources. The minimum capacity requirement of the storage supercapacitor is given by equation:

$$C_{SCAP-\min} = \frac{\Delta T \times I_{AVG}}{\Delta V_{CAP}} \tag{2}$$

where I_{AVG} is the average current that consumed by the sensor circuit, ΔT presents the time period of the operational phase, and ΔV_{CAP} denotes the maximum voltage change of the supercapacitor during the operation, corresponding to the difference between V_{HTHR} and V_{LTHR} in the worst-case scenario.

To guarantee that electricity is properly distributed from the energy harvester block to the sensor part, the power supervisory unit serves as an intermediary [29]. To fulfill this role, an ultralow profile load switch (nRF-PPK2, Nordic Semiconductor) is integrated into the supervisory scheme. The voltage across the supercapacitor (V_{HTHR}) is continuously measured by this power supervisory unit and the associated control signal, V_{CTR}, is produced by comparing it to specified voltage thresholds (V_{LTHR} and V_{LTHR}). Specifically, when V_{HAR} exceeds the high-voltage threshold, the control signal V_{CTR} activates the load switch, enabling power delivery to the load. Conversely, when V_{HAR} falls below the low-voltage threshold, the control signal V_{CTR} deactivates the switch, thereby interrupting the power supply to the load.

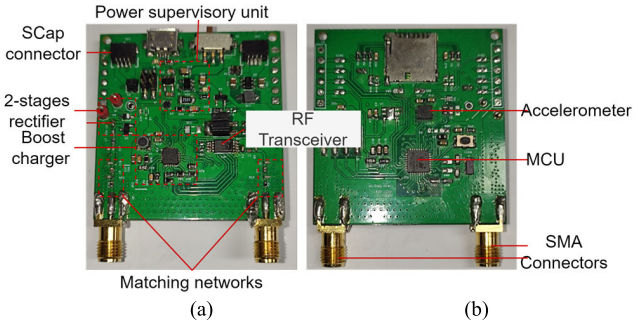

FIGURE 5. The prototype of the proposed batteryless sensor tag: (a) The top view of the circuit, (b) Bottom view of the circuit.

C. SENSOR MODULE DESIGN

To quantify dairy cow behaviors, the sensor module incorporates the ADXL362 three-axis accelerometer from analog devices. This accelerometer achieves exceptional power efficiency, consuming a mere 1.7 μA at a 10 Hz data sampling rate. Further, its wide operating voltage range of 1.8–3.3 V provides flexibility in terms of power-supply options, making it suitable for various application scenarios. The accelerometer also features an output-data-rate selection capability, allowing convenient customization to meet specific application requirements. Furthermore, in standby mode, it exhibits an impressively low current draw of only 10 nA, significantly reducing power consumption at the system level.

The sensor module's central component is the STM32L432 ultralow-power microcontroller from ST Microelectronics, chosen for its exceptional performance. Operating within a wide power-supply range of 1.17 – 3.9 V, the microcontroller offers versatile power-supply options. Notably, its current consumption is remarkably low, measuring at 81 μA/MHz in run mode. The microcontroller's power consumption drops even more to an astounding 28 nA when it is in standby mode with the real-time clock capability. The microcontroller incorporates an advanced, adaptive real-time accelerator, enabling zero-wait-state execution and effectively optimizing power efficiency.

For wireless communication between the reader and sensor tags, a backscatter communication link is established, minimizing the hardware size and power consumption. The chosen tag chip is the EM4325 from EM Microelectronics,

which runs at ultrahigh frequencies (860-960 MHz) and complies with the EPC RFID protocols. The tag chip's memory allows read or write operations even in sleep mode, providing energy-saving advantages. Additionally, the backscatter technology eliminates the need for the tag chip to supply power for backscattering data to the reader. Seamless integration with the microcontroller is achieved through the serial peripheral interface, and the microcontroller can reduce current consumption as low as 1.8 μA in deep sleep mode.

D. PCB-SENSOR TAG PERFORMANCE EVALUATION

1) RFEH EVALUATION METRIC

In this study, a critical metric known as RF-DC conversion efficiency (PCE) is analyzed. This metric quantifies the portion of power the antenna receives that is effectively transferred through the rectifying circuit and applied to the load [30]. The efficiency is expressed as follows:

$$\eta_{RF-DC} = \frac{P_{dc}}{P_{in}} \tag{3}$$

where P_{in} denotes the input RF power received by the antenna, and P_{dc} denotes the DC power at the output of the rectifier over a known load. The load impedance is calculated based on the sensor module's power requirements. The sensor module's current consumption changes in accordance with its operating condition, which also affects the related load impedance. The impedance corresponding to the state with the lowest current consumption was chosen to ensure that the sensor tag could continue to scavenge energy from environment.

To evaluate the efficiency, the values of P_{dc} (power delivered to the load) and P_{in} (input power) in Eq. (3) were determined. For measuring Pin at a specific distance from the reader, the PCB-printed antenna was initially connected to a N9320A spectrum analyzer from Keysight Technologies. Subsequently, the output voltage of the rectifier was measured using a multimeter with the sensor tag placed at the same distance, allowing for the computation of the output power. The distance varied between 0.1 and 4 meters.

For this experiment, a Speedway R700 reader (Impinj, USA) was employed, with the output RF radiation set at the maximum of 33 dBm. The reader works with the EPC gen 2 interface protocol for the UHF RFID band. It has a maximum receiver sensitivity of −92 dBm (corresponding to the distance of 12 meters) and can read up to 1100 tags per second, demonstrating its excellent performance. Additionally, the reader has an Ethernet connection that enables accessible data streaming from the sensor tag to the main computer. The reader was attached to an S8658WPR 6.3 dBi circularly polarized antenna in order to transmit RF signals to the surrounding environment.

2) ENERGY HARVESTING PERFORMANCE

The evaluation of the harvesting system primarily focused on two key factors: efficiency and sensitivity of RF-DC conversion [31]. A variety of input RF powers, from -8 dBm to 11.5 dBm, are shown in Fig. 6 together with the measured rectifying voltage and the related RF-to-DC conversion efficiency. Notably, there is a decrease in the rectifying voltage as the input power decreases. The highest conversion efficiency of 58.76% is achieved at an input RF power of -3.5 dBm. Conversely, the lowest efficiency of 5% is observed at the highest input power when the harvester is positioned 50 cm away from the reader. These findings provide substantial evidence supporting the feasibility of the proposed design for applications with low RF power density.

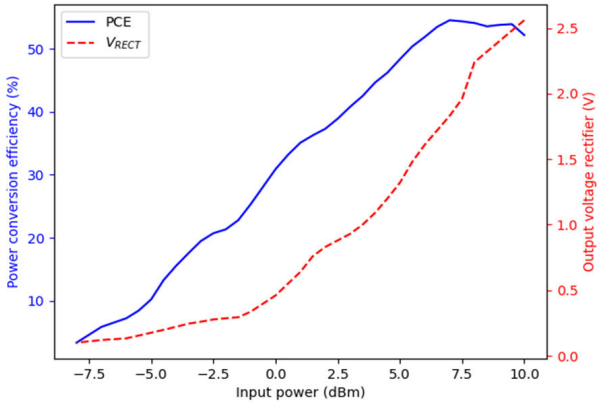

FIGURE 6. The efficiency of the RF energy harvester's power conversion and the rectifying voltage it produces in accordance with the RF power input.

Furthermore, the harvesting sensitivity was determined to be -7.5 dBm through experimental evaluation, resulting in a rectifying voltage of 380 mV or 18.36 W. Figure 6 illustrates the measured rectifying voltage and the corresponding RF-to-DC conversion efficiency for an input RF power range of -7.53 to 10.16 dBm, which corresponds to distances ranging from 1.5 to 6 m. The RF-energy-harvester module's efficiency curves and input power exhibit similar patterns. The harvester achieves its highest Power Conversion Efficiency (PCE) of 65.04% with a rectifying output voltage of 1.65 V at a distance of 2.5 m. Conversely, the lowest efficiency of 25.5% is observed at the lowest input power when the harvester is placed 6 m away from the reader. The fully charging time of the sensorr tag is 5 minutes at distance of 2.5 metter.

3) SAMPLING FREQUENCY OF ACCELEROMETER SELECTION

The power consumption of the circuit is partially influenced by sampling rate of the accelerometer, with higher frequencies requiring higher currents and lower frequencies resulting in reduced current consumption. Table 2 provides the current consumption values for different accelerometer sampling frequencies. Previous studies have utilized various sampling frequencies, ranging from a high level of 50 Hz [32] to moderate ones of 25 Hz [33], 10 Hz [34], and even as low as 1 Hz [35]. In order to achieve a balance between the data sampling capabilities and the power consumption of device, we opted for a sampling rate of 10 Hz.

TABLE 2. The power consumption of the sensor tag at different sampling rates.

Sampling rate (Hz)	Current consumption (μA)
50	252.5
20	111.6
10	51.07
1	4.9

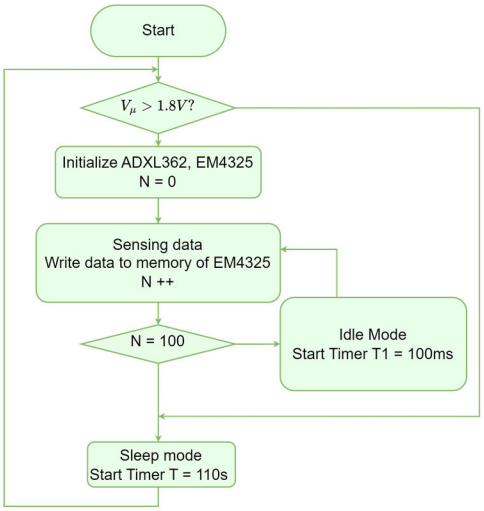

FIGURE 7. Time operation algorithm of the sensor tag.

4) REDUCING CURRENT CONSUMPTION

In order to reduce the average current consumption of the sensor tag, two critical factors must be optimized by well-designed software programming: T_{ACT} and I_{ACT}. Additionally, hardware modifications can help reduce I_{SL}. Among the three components of the circuit, the transceiver exhibits the highest current consumption during the sleep phase. To address this issue, a solution is implemented by switching the RF transceiver to passive mode once it receives data from the microcontroller. This effectively isolates the RF transceiver from the circuit. The operational algorithm of the sensor tag is illustrated in Fig. 7.

The sensor module incorporates a Texas Instruments TPS22916 low leakage load switch, acting as an intermediary between the RF transceiver and the power supply line. This switch boasts an exceptionally low current leakage rate. Controlled by the host microcontroller, the switch is activated by a high logic signal, facilitating the connection between the RF transceiver and the sensor module. Conversely, the switch disconnects the sensor module from the RF transceiver upon receiving a low logic signal from the microcontroller.

The sensor module operates in two distinct phases: active mode and sleep mode. During the initial phase, the microcontroller and accelerometer remain active, while the RF transceiver remains in sleep mode. The accelerometer takes measurements, and the microcontroller processes the gathered data. Subsequently, the microcontroller transfers the processed data to the user memory of the RF transceiver, which remains in sleep mode during this period.

Conversely, in the sleep phase, the sensor tag's power consumption is significantly reduced by turning the microcontroller and the accelerometer into standby mode. The RF transceiver continues to remain in sleep mode. To commence the next operational cycle, the microcontroller is awakened by an interruption generated at predetermined intervals by its real-time clock. This mechanism ensures that the desired sampling rate is maintained while conserving power during the sleep phase.

The current contribution in active mode can be described using the following formula according to the sensor tag's operating algorithm:

$$I_{ACT} = I_{MCU-A} + I_{ACC-A} + I_{RF-A} \tag{4}$$

where I_{MCU-A}, I_{ACC-A}, and I_{RF-A} are the power consumption of host microcontroller, accelerometer component, and the RF transceiver in active mode respectively.

While in sleep mode, the power consumption by the module is determined by:

$$I_{SL} = I_{MCU-S} + I_{RF-S} \tag{5}$$

where I_{MCU-S} is the current of the microcontroller in sleep mode and I_{RF-S} is the current consumed in standby mode.

follow the operating algorithm as shown in Fig. 7, each duty cycle of the microcontroller includes 2 periods: the active phase and sleep phases. To ensure accurate measurement of these currents, a power shield (NRF-PPK2, Nordic Semiconductor) with the capability of detecting currents as small as nA is utilized. The measured results serve to determine the parameters in equations (4) and (5) as follows: I_{ACT} = 365.6 μA, T_{ACT} = 16 ms, I_{SL} = 0.675 μA, and ISL = 100 ms. Subsequently, the average current consumption (I_{AVG}) is calculated to be 51.04 μA as shown in table 2 at sampling rate 10 Hz.

III. EXPERIMENT AND ANALYSIS

A. EXPERIMENT SETUP

An experiment was conducted at Tan Tai Loc dairy farm in Soc Trang, Vietnam, (9°31'42.1''N, 105°54'08.7''E). This privately owned farm covers an area exceeding 190 m2, as depicted in Fig. 9. The experiment focused on behavioral monitoring and involved 18 dairy cattle aged three years or older. The sensor tag was attached to the cow's collar as depicted in Fig. 8. The reader and antenna are located in front of the warehouse, at the top (Fig. 9), while the server is located in the control room.

The duration of the experiment was two weeks, during which we observed and monitored four specific behaviors exhibited by the cattle: grazing, walking, standing, and ruminating. The definition of a description of four behavior as well as the number of collected samples of each type, are shown in Table 3. To capture and document the activities of the cattle, we employed six internet protocol cameras. This camera

FIGURE 8. Sensor mounted on the cow's neck and the position of the reader.

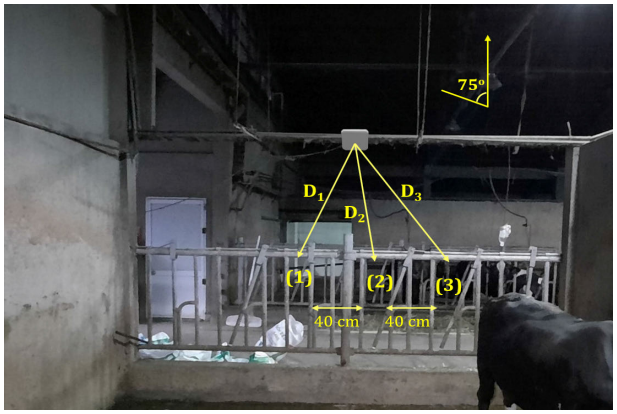

FIGURE 9. Time operation algorithm of the sensor tag.

setup included four RGB cameras strategically positioned within four sub-barns, as well as two others situated in the grazing area. To ensure the utmost accuracy and reliability of the collected data, we enlisted the assistance of four experienced dairy farmers who conducted manual observations in conjunction with the camera based monitoring approach.

Accurate cattle behavior classification relies on a well-curated dataset that captures the diverse range of behaviors exhibited by the animals [36]. Data acquisition was conducted three times daily to capture the acceleration data of the dairy cattle following their aeting period. During the initial two data collection sessions, the sensor tag continuously recorded the cow's behaviors for 90 min. In the third data-collection session, the sensor was attached to the cow's neck. The dairy farm comprised small barns, each accommodating three to four cattle. For this study, four barns were utilized, with three cattle housed together in each barn. Each cow had an assigned feeding position and received meals at three specific times: 6:30 in the morning, 12:30 at noon, and 16:00 in the afternoon. After 18:30, the barns were secured to provide the dairy cattle with a period of rest. Observations and recordings of dairy cow behaviors were conducted consistently over 14 continuous days.

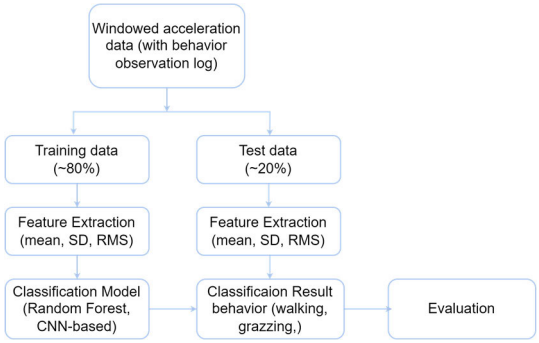

FIGURE 10. Data preprocessing pipeline.

TABLE 3. Description of the observed behaviors and the number corresponding of samples.

Label	Number of samples	Description
Standing	9450	The dairy cow resting on standing status.
Walking	56015	The free movement of a dairy cow from one position to another continuously.
Grazing	64015	The dairy cow eat grass without raising its head.
Ruminating	7150	The dairy cow re-chewing, and re-swallowing feed.

In the conducted experiment, the cattle were granted freedom to graze in a designated area. To maintain their health and well-being, a veterinary monitoring program was implemented. The data-acquisition process involved configuring the sampling rate to 10 Hz, the conversion precision to 16 bits, and the range to $\pm$ 4 g, resulting in a noise floor of 0.5 mg. For data recording, a microcontroller and a local storage device were utilized.

During the experiment, the sensor device was securely affixed to the cow's neck using a dedicated nylon collar belt. Positioning the sensors around the collar area is a common practice in cow behavior monitoring studies to mitigate the risk of the sensors being chewed on and to accommodate appropriately sized batteries. The tightness of the collar was adjusted to ensure optimal acceleration coupling in response to the cow's natural movements while minimizing any discomfort caused to the animal.

B. DATA PREPROCESSING

Table 4 displays the class label, descriptions, and available sample counts for four prominent behaviors, along with example video frames. These behaviors encompass the most frequently observed activities in the daily routines of the cattle. Notably, even subtle variations in their distribution can provide insights into subclinical or ''hidden'' diseases. Less common behaviors were excluded from the analysis to focus on the significant ones. The proposed recognition process is illustrated in Fig. 10. The data from the accelerometer

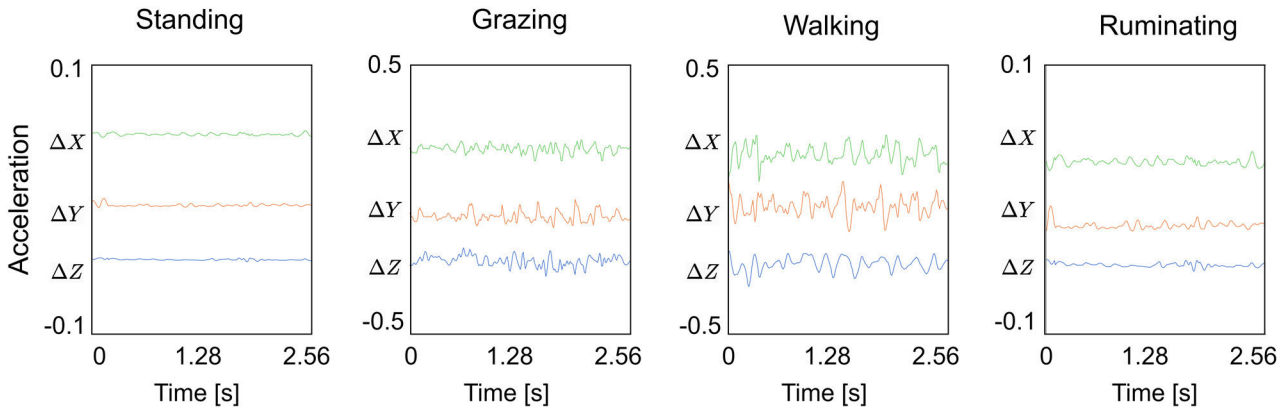

FIGURE 11. The waveforms of four different observed behaviors including standing, grazing walking and ruminating.

were divided into windows of a fixed length of 2.56 s or 256 samples per window. These segmented data served as the input for the classification models. Data that has been labeled is based on observations of dairy cow activity made by security cameras.

The training data consisted of approximately 60% randomly selected samples from the complete dataset, while the remaining data were allocated for testing purposes. 20% of the training dataset was used for validating. This division proved to be effective in accurately classifying cow behaviors. The classification model was trained using the labeled training data, utilizing the proposed feature set. Subsequently, the test data were labeled using this trained classification model. The resulting classification results, representing the predicted behaviors as labeled by the model, were evaluated by comparing them with the actual behavior observation results.

C. DEEP LEARNING MODEL FOR COW BEHAVIOR CLASSIFICATION

Machine learning techniques, especially neural networks, have been proven to be effective in behavioral classification tasks using the IMU data, both in human and animal contexts. Xia et al. [37] proposed the LSTM-CNN Architecture for human activity recognition (HAR) task with six different activity classes. In physical behavioral studies, IMU data, which captures accelerations and angular velocities, has been harnessed to discern various activities such as walking, running, and posture changes. Deep learning methodologies have proven particularly adept in processing the intricate patterns within IMU data, offering a non-intrusive means of understanding human behavior. Parallelly, in the domain of animal behavior classification, especially in livestock like cattle, IMU data has been instrumental in deciphering activities like grazing, standing, or resting. The application of machine learning and neural networks to IMU data in these studies has enabled the automated identification and categorization of diverse behaviors, facilitating advancements in precision livestock farming and animal welfare monitoring.

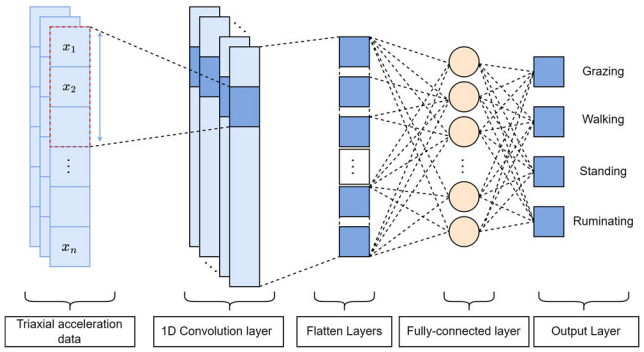

FIGURE 12. The architecture of the proposed 1D-CNN model for cow behavior classification.

Effective monitoring and management of cattle depends on the precise behavior of classification model. This section introduces the cow-behavior classification using the Bi-LSTM deep learning model. Additionally, we constructed other classification models, namely 1D-CNN, MLP, and SVM, to enable a comparative evaluation of their effectiveness. Detailed descriptions of the architectures for each of these classification models are presented as follows.

1) ONE-DIMENSIONAL CNN MODEL

The one-dimensional convolutional neural network (1D-CNN) [38] model is a powerful tool for classifying behaviors based on the data collected from the neck-mounted sensor tag. This model leverages the spatial correlation of the data to capture relevant features and make accurate predictions. The input of the 1D-CNN model consists of the acceleration data collected over a window of 12 s. Each window is treated as a single channel, and the model applies convolutional filters across the time dimension to capture local patterns. Thereafter, the output of the convolutional layers is passed through max-pooling layers to downsample the data and reduce dimensionality.

Following the convolutional and pooling layers, fully connected layers are employed to learn higher-level

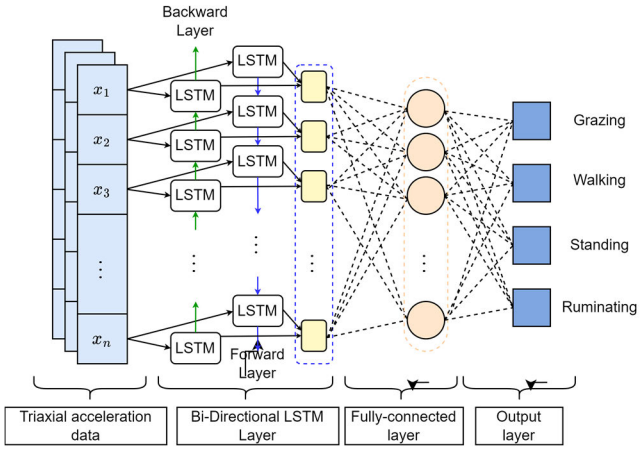

FIGURE 13. The architecture of the proposed Bi-LSTM model for cow behavior classification.

representations and make behavioral predictions. The number of neurons in the fully connected layers and the activation functions are carefully tuned to optimize the performance of the model. To prevent overfitting, dropout layers are incorporated between the fully connected layers, which randomly disable a portion of the neurons during training.

The model is trained using a labeled dataset of cow behaviors, including standing, walking, and grazing. The training is performed using an optimization algorithm to minimize the categorical cross-entropy loss function. The model parameters are updated iteratively using backpropagation, and the process continues until convergence is achieved.

2) BI-DIRECTIONAL LSTM MODEL

The Bi-LSTM [39] model extends the capabilities of the traditional LSTM network by incorporating bidirectional processing of sequential data. While standard LSTM networks consider only the past context, Bi-LSTM networks leverage both past and future context to capture dependencies in both directions. The advantage of LSTM is that it can recognize long-term dependencies.

The Bi-LSTM model is utilized as an effective tool for cow-behavior classification based on the acceleration data obtained from the neck-mounted sensor tag. This model is particularly suitable for capturing temporal dependencies and long-range dependencies in sequential data. The input of the Bi-LSTM model consists of the acceleration data collected over a window of 2.56 s. Each data point in the sequence represents the acceleration magnitude at a specific time step. The Bi-LSTM model processes the sequential data bidirectionally, using both forward and backward LSTM layers. This allows the model to capture contextual information from past and future time steps simultaneously. Each layer of the Bi-LSTM neural network is made up of a forward and a backward recurrent network for multilayer stacking. The output results of the forward and backward LSTMs from the previous layer are combined and transferred to the following layer of the network.

To prevent overfitting, dropout layers are incorporated between the LSTM and fully connected layers. The dropout layer randomly disables a portion of the neurons during training, which encourages the model to learn more robust and generalizable representations. The Bi-LSTM model is trained using a labeled dataset of cow behaviors, including standing, walking, and grazing. The training process involves optimizing the model parameters to minimize the categorical cross-entropy loss function. Backpropagation is employed to update the model's parameters iteratively, allowing it to learn and adapt to the behavior patterns present in the data.

3) MUTILAYERS PERCEPTRON MODEL

Before the introduction of CNN as a highly effective machine learning model, MLP networks were considered state-of-the-art. MLP models differ from CNN models in that they consist only of fully connected layers and an output layer, requiring a significant number of parameters for their development. For the acceleration dataset, we constructed an MLP model with two hidden layers, consisting of 256 and 128 nodes, respectively. To mitigate the risk of overfitting, a dropout rate of 50% was implemented in the MLP model. The Adam algorithm was chosen as the optimizer, while the cross-entropy loss function was employed for this model, similar to the earlier models.

4) SUPPORT VECTOR MACHINE

To compare the model's performance with those of deep-learning models, an SVM model was employed. SVMs are nonparametric models that address multiclass classification problems through either the one-vs-all or one-vs-one strategy. Unlike deep-learning models, SVM does not require extensive parameter tuning and is suitable for small datasets with few outliers. However, the computational cost of SVM increases linearly with the number of classes. In this study, three SVM binary classifiers were utilized to identify three distinct acceleration states. The radial basis function was selected as the kernel for the SVM model.

5) MODEL EVALUATION METRIC

After learning was completed, the effectiveness of the classifier model was examined based on an independent test set. To evaluate the proposed models, the confusion matrix was used to calculate the accuracy, sensitivity, specificity, and Matthews correlation coefficient (MCC) using the following formulas:

$$Accuracy = \frac{TP}{TP + TN + FP + FN} \tag{6}$$

$$Sensitivity = \frac{TP}{TP + FN} \tag{7}$$

$$Specitivity = \frac{TP}{TN + FP} \tag{8}$$

$$MCC = \frac{TP \times TN - FP \times FN}{\sqrt{(TP + Fp)(Tp + FN)(TN + FP)(TN + FN)}} \tag{9}$$

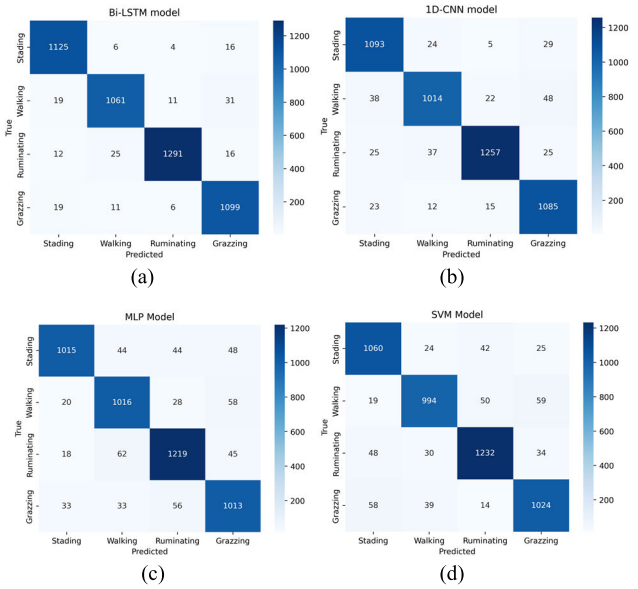

FIGURE 14. The proposed architecture of 1D-CNN model for cow behavior classification.

In classification problems, employing cross-validation techniques aids in preventing overfitting when predicting on test sets. This approach also serves as a strategy for optimizing hyperparameters in deep-learning models. For our study, we utilized fivefold cross-validation to assess the performance of all proposed models, including LSTM, CNN, MLP, and SVM. The fivefold average accuracy was used to select the most suitable architecture for each model. To ensure complete utilization of the training set and avoid missing data, the entire training set was employed during training. To select the best-performance weight set, the early stopping technique was implemented. All models were constructed, trained, and evaluated using Python and the TensorFlow framework.

IV. RESULT

To evaluate the effectiveness of our self-powered cattle behavior monitoring system, we conducted extensive data measurement and analysis. In this section, we present the results obtained from the sensor nodes deployed on cattle and highlight the insights gained through the analysis of behavior data from the classification result.

A. BEHAVIOR MEASUREMENT

In line with the aforementioned details, the experiment focuses on measuring four distinct behaviors: walking, standing, grazing, and ruminating. To monitor the acceleration changes, the battery-less sensor tag is securely attached to the cow's collar. The acceleration data is recorded at one-minute intervals. Fig. 11 illustrates the data logger and the corresponding raw time series data. These segmented data serve as input for the classification models employed in the study.

TABLE 4. Classification result with bi-LSTM model.

Label	Precision	Recall	F1 Score
Standing	96.23%	95.39%	95.80%
Walking	94.46%	94.04%	94.24%
Grazing	98.78%	97.53%	98.15%
Ruminating	95.58%	97.45%	96.50%

B. CLASSIFICATION RESULT

The accuracies of the four models in classifying each behavior were evaluated using a confusion matrix. A confusion matrix is a square matrix that provides a visual representation of the performance of a classification system with multiple classes. It consists of two dimensions: one dimension represents the actual classes (true class), whereas the other represents the classes predicted by the model (predicted class). The results of the confusion matrix for the Bi-LSTM and 1D-CNN models are depicted in Figs. 14(a) and (b), respectively. Both models exhibited misclassification rates in the classification between the grazing behavior and the walking behavior. For the 1D-CNN model, this misclassification rate reached 6.22%, whereas for the Bi-LSTM model, it was 3.31%.

Table 4 shows the overall accuracy comparison among the four kinds of behaviors with the LSTM models. The overall accuracy achieved for all four behaviors was more than 95% and the best performance reached 98.78% in grazing class. Overall, the two proposed deep-learning models are superior to the traditional machine learning algorithms, including the SVM and MLP models.

In the realm of time-series classification tasks, particularly in the nuanced domain of cow behavior data analysis, the superiority of the Bi-Long Short-Term Memory (Bi-LSTM) model becomes evident. Unlike conventional neural network models, Bi-LSTM excels in capturing intricate temporal dependencies inherent in time-series datasets, a critical aspect when deciphering the nuanced behaviors of cattle over time. The sequential nature of cow behavior data necessitates a model capable of retaining and leveraging information from past observations, and the inherent architecture of Bi-LSTM, featuring memory cells and input, forget, and output gates, positions it as exceptionally adept in modeling such complex temporal dynamics. Through our rigorous experimentation and comparative analysis, the Bi-LSTM model consistently outperformed other neural network counterparts in accurately classifying and predicting various cattle behaviors. This enhanced capability not only bolsters the reliability of our monitoring system but also reaffirms the Bi-LSTM model's superiority in discerning intricate patterns within time-series datasets, thereby solidifying its position as a formidable choice for the classification of cow behavior data in our proposed self-powered system.

V. CONCLUSION

This study represents a proof-of-concept for a self-powered cow monitoring system leveraging RF energy-harvesting technology for the classification of cow behavior in a smart dairy farm setting. Central to this system is a neck-mounted sensor tag device powered by RF energy and equipped with an accelerometer. The sensor tag exhibited a noteworthy PCE exceeding 58.76% when supplied with an input RF power of 7 dBm, and the total charging time with a 10-mF supercapacitor is 5 minutes. Remarkably, it sustained uninterrupted operation for over 90 minutes without the need for recharging. Furthermore, the sensor tag's current profiles showcased its adaptability to applications characterized by ultralow power consumption.

To evaluate the feasibility of this self-powered dairy-cow-monitoring system in real-world scenarios, a two-week-long demonstration was conducted. The system successfully classified three recognized states of the cow's behavior. Two deep-learning models were developed to classify these states using the data collected during the experiment. The results indicated that both models effectively classified the three dairy cow behaviors, with the highest accuracy achieved for the walking behavior. Among the models, the Bi-LSTM model outperformed the 1D-CNN model and other traditional methods, achieving an overall accuracy of 96.76%.

While the behavior data measurement results are promising, there are certain limitations to consider. The accuracy of behavior classification can be further improved by collecting more diverse and extensive datasets, accounting for variations among different cattle breeds and individual characteristics. Additionally, incorporating additional sensor modalities and advanced data fusion techniques may enhance the system's ability to capture a broader range of behaviors.

In conclusion, the behavior data measurement results obtained from our self-powered cattle behavior monitoring system demonstrate its effectiveness in capturing and analyzing cattle behaviors. The combination of accurate behavior classification using the Bi-LSTM neural network and energy-efficient data collection through radio frequency energy harvesting establishes the system as a valuable tool for real-time monitoring and managing cattle behavior in agricultural settings. By harnessing RF energy harvesting, our system has the potential to operate permanently, eliminating the need for frequent battery replacements and thereby mitigating associated expenses. This not only offers a substantial economic advantage but also enhances the sustainability of the monitoring solution. Future work will focus on optimizing the rectifier will be to enhance the PCE, reducing the charging time and increasing its capacity to extend the usage time of the sensor tag.

REFERENCES

[1] J. A. Jacobs and J. M. Siegford, "Invited review: The impact of automatic milking systems on dairy cow management, behavior, health, and welfare," *J. Dairy Sci.*, vol. 95, no. 5, pp. 2227–2247, May 2012.

[2] H. Lee, S. A. Kim, S. Coakley, P. Mugno, M. Hammarlund, M. A. Hilliard, and H. Lu, "A multi-channel device for high-density target-selective stimulation and long-term monitoring of cells and subcellular features in C. Elegans," *Lab Chip*, vol. 14, no. 23, pp. 4513–4522, 2014.

[3] E. Vasseur, "Animal behavior and well-being symposium: Optimizing outcome measures of welfare in dairy cattle assessment," *J. Animal Sci.*, vol. 95, no. 3, p. 1365, 2017.

[4] M. Fadul, L. D'Andrea, M. Alsaaod, G. Borriello, A. Di Lori, D. Stucki, P. Ciaramella, A. Steiner, and J. Guccione, "Assessment of feeding, ruminating and locomotion behaviors in dairy cows around calving—A retrospective clinical study to early detect spontaneous disease appearance," *PLoS ONE*, vol. 17, no. 3, Mar. 2022, Art. no. e0264834.

[5] E. Trevisi, A. Zecconi, S. Cogrossi, E. Razzuoli, P. Grossi, and M. Amadori, "Strategies for reduced antibiotic usage in dairy cattle farms," *Res. Veterinary Sci.*, vol. 96, no. 2, pp. 229–233, Apr. 2014.

[6] L.-G. Tran, H.-K. Cha, and W.-T. Park, "RF power harvesting: A review on designing methodologies and applications," *Micro Nano Syst. Lett.*, vol. 5, no. 1, pp. 1–16, Dec. 2017.

[7] H.-J. Kim, H. Hirayama, S. Kim, K. J. Han, R. Zhang, and J.-W. Choi, "Review of near-field wireless power and communication for biomedical applications," *IEEE Access*, vol. 5, pp. 21264–21285, 2017.

[8] P. S. Yedavalli, T. Riihonen, X. Wang, and J. M. Rabaey, "Far-field RF wireless power transfer with blind adaptive beamforming for Internet of Things devices," *IEEE Access*, vol. 5, pp. 1743–1752, 2017.

[9] J. A. Shaw, "Radiometry and the Friis transmission equation," *Amer. J. Phys.*, vol. 81, no. 1, pp. 33–37, Jan. 2013.

[10] B. Robert, B. J. White, D. G. Renter, and R. L. Larson, "Evaluation of three-dimensional accelerometers to monitor and classify behavior patterns in cattle," *Comput. Electron. Agricult.*, vol. 67, nos. 1–2, pp. 80–84, Jun. 2009.

[11] J. A. V. Diosdado, Z. E. Barker, H. R. Hodges, J. R. Amory, D. P. Croft, N. J. Bell, and E. A. Codling, "Classification of behaviour in housed dairy cows using an accelerometer-based activity monitoring system," *Animal Biotelemetry*, vol. 3, no. 1, pp. 1–14, Dec. 2015.

[12] K. Džermeikaitė, D. Bačėninaitė, and R. Antanaitis, "Innovations in cattle farming: Application of innovative technologies and sensors in the diagnosis of diseases," *Animals*, vol. 13, no. 5, p. 780, Feb. 2023.

[13] A. A. Babayo, M. H. Anisi, and I. Ali, "A review on energy management schemes in energy harvesting wireless sensor networks," *Renew. Sustain. Energy Rev.*, vol. 76, pp. 1176–1184, 2017.

[14] H.-D. Do, D.-E. Kim, M. B. Lam, and W.-Y. Chung, "Self-powered food assessment system using LSTM network and 915 MHz RF energy harvesting," *IEEE Access*, vol. 9, pp. 97444–97456, 2021.

[15] P. Martiskainen, M. Järvinen, J.-P. Skön, J. Tiirikainen, M. Kolehmainen, and J. Mononen, "Cow behaviour pattern recognition using a three-dimensional accelerometer and support vector machines," *Appl. Animal Behav. Sci.*, vol. 119, nos. 1–2, pp. 32–38, Jun. 2009.

[16] G. Fortino, R. Giannantonio, R. Gravina, P. Kuryloski, and R. Jafari, "Enabling effective programming and flexible management of efficient body sensor network applications," *IEEE Trans. Human-Mach. Syst.*, vol. 43, no. 1, pp. 115–133, Jan. 2013.

[17] B. Wang, P. Dehghanian, S. Wang, and M. Mitolo, "Electrical safety considerations in large-scale electric vehicle charging stations," *IEEE Trans. Ind. Appl.*, vol. 55, no. 6, pp. 6603–6612, Nov. 2019.

[18] M. W. Gardner and S. R. Dorling, "Artificial neural networks (the multilayer perceptron)—A review of applications in the atmospheric sciences," *Atmos. Environ.*, vol. 32, nos. 14–15, pp. 2627–2636, Aug. 1998.

[19] S. Suthaharan, "Support vector machine," in *Machine Learning Models and Algorithms for Big Data Classification* (Integrated Series in Information Systems), vol. 36. Boston, MA, USA: Springer, 2016, doi: 10.1007/978-1-4899-7641-3_9.

[20] T. Soyata, L. Copeland, and W. Heinzelman, "RF energy harvesting for embedded systems: A survey of tradeoffs and methodology," *IEEE Circuits Syst. Mag.*, vol. 16, no. 1, pp. 22–57, 1st Quart., 2016.

[21] B. Liu, H. Aliakbarian, Z. Ma, G. A. E. Vandenbosch, G. Gielen, and P. Excell, "An efficient method for antenna design optimization based on evolutionary computation and machine learning techniques," *IEEE Trans. Antennas Propag.*, vol. 62, no. 1, pp. 7–18, Jan. 2014.

[22] C. M. Kruesi, R. J. Vyas, and M. M. Tentzeris, "Design and development of a novel 3-D cubic antenna for wireless sensor networks (WSNs) and RFID applications," *IEEE Trans. Antennas Propag.*, vol. 57, no. 10, pp. 3293–3299, Oct. 2009.

[23] H. F. Pues and A. R. Van de Capelle, "An impedance-matching technique for increasing the bandwidth of microstrip antennas," *IEEE Trans. Antennas Propag.*, vol. 37, no. 11, pp. 1345–1354, Nov. 1989.
[24] R. E. Barnett, J. Liu, and S. Lazar, "A RF to DC voltage conversion model for multi-stage rectifiers in UHF RFID transponders," *IEEE J. Solid-State Circuits*, vol. 44, no. 2, pp. 354–370, Feb. 2009.
[25] C. R. Valenta and G. D. Durgin, "Harvesting wireless power: Survey of energy-harvester conversion efficiency in far-field, wireless power transfer systems," *IEEE Microw. Mag.*, vol. 15, no. 4, pp. 108–120, Jun. 2014.
[26] D. Jayawardana, S. Kharkovsky, R. Liyanapathirana, and X. Zhu, "Measurement system with accelerometer integrated RFID tag for infrastructure health monitoring," *IEEE Trans. Instrum. Meas.*, vol. 65, no. 5, pp. 1163–1171, May 2016.
[27] G. Kazdaridis, N. Sidiropoulos, I. Zografopoulos, and T. Korakis, "EWake: A novel architecture for semi-active wake-up radios attaining ultra-high sensitivity at extremely-low consumption," 2021, *arXiv:2103.15969*.
[28] W. Liu, K. Huang, X. Zhou, and S. Durrani, "Next generation backscatter communication: Systems, techniques, and applications," *EURASIP J. Wireless Commun. Netw.*, vol. 2019, no. 1, pp. 1–11, Mar. 2019.
[29] F. T. Ulaby, W. H. Stiles, and M. Abdelrazik, "Snowcover influence on backscattering from terrain," *IEEE Trans. Geosci. Remote Sens.*, vol. GE-22, no. 2, pp. 126–133, Mar. 1984.
[30] D. Khan, S. J. Oh, K. Shehzad, M. Basim, D. Verma, Y. G. Pu, M. Lee, K. C. Hwang, Y. Yang, and K.-Y. Lee, "An efficient reconfigurable RF-DC converter with wide input power range for RF energy harvesting," *IEEE Access*, vol. 8, pp. 79310–79318, 2020.
[31] L. Svilainis, V. Dumbrava, and A. Chaziachmetovas, "Universal acquisition system for frequency domain parameters measurement," in *Proc. 6th IEEE Int. Conf. Intell. Data Acquisition Adv. Comput. Syst.*, vol. 1, Sep. 2011, pp. 10–15.
[32] V. Bloch, L. Frondelius, C. Arcidiacono, M. Mancino, and M. Pastell, "Development and analysis of a CNN- and transfer-learning-based classification model for automated dairy cow feeding behavior recognition from accelerometer data," *Sensors*, vol. 23, no. 5, p. 2611, Feb. 2023.
[33] D.-N. Tran, T. N. Nguyen, P. C. P. Khanh, and D.-T. Tran, "An IoT-based design using accelerometers in animal behavior recognition systems," *IEEE Sensors J.*, vol. 22, no. 18, pp. 17515–17528, Sep. 2022.
[34] W. Shen, F. Cheng, Y. Zhang, X. Wei, Q. Fu, and Y. Zhang, "Automatic recognition of ingestive-related behaviors of dairy cows based on triaxial acceleration," *Inf. Process. Agricult.*, vol. 7, no. 3, pp. 427–443, Sep. 2020.
[35] L. Schmeling, G. Elmamooz, P. T. Hoang, A. Kozar, D. Nicklas, S. Thurner, and E. Rauch, "Training and validating a machine learning model for the sensor-based monitoring of lying behavior in dairy cows on pasture and in the barn," *Animals*, vol. 11, no. 9, p. 2660, Sep. 2021.
[36] S. Gupta, M. S. Mortensen, S. Schjørring, U. Trivedi, G. Vestergaard, J. Stokholm, H. Bisgaard, K. A. Krogfelt, and S. J. Sørensen, "Amplicon sequencing provides more accurate microbiome information in healthy children compared to culturing," *Commun. Biol.*, vol. 2, no. 1, p. 291, Aug. 2019.
[37] K. Xia, J. Huang, and H. Wang, "LSTM-CNN architecture for human activity recognition," *IEEE Access*, vol. 8, pp. 56855–56866, 2020, doi: 10.1109/ACCESS.2020.2982225.
[38] S. Kiranyaz, O. Avci, O. Abdeljaber, T. Ince, M. Gabbouj, and D. J. Inman, "1D convolutional neural networks and applications: A survey," *Mech. Syst. Signal Process.*, vol. 151, Apr. 2021, Art. no. 107398.
[39] S. Siami-Namini, N. Tavakoli, and A. S. Namin, "The performance of LSTM and BiLSTM in forecasting time series," in *Proc. IEEE Int. Conf. Big Data (Big Data)*, Dec. 2019, pp. 3285–3292.

THAI HA DANG received the B.E. degree in control engineering and automation from Hanoi University of Science and Technology, Vietnam, in 2021. He is currently a pursuing the M.S. degree with the Department of AI Convergence, Pukyong National University, Busan, South Korea. His research interests include wireless sensors networks, RF energy harvesting, and machine learning on embedded devices.

LIONEL NKENYEREYE received the B.S. degree in data communication from the High Institute of Technology, Burundi, in 2005, and the M.S. and Ph.D. degrees in computer engineering from Dong-Eui University, South Korea, in 2016 and 2019, respectively. He was a Postdoctoral Fellow Researcher with Sejong University, Seoul, South Korea, from 2019 to 2020. He has been a Postdoctoral Fellow with Pukyong National University, Busan, South Korea, since July 2021. His research interests include vehicle-to-everything communication, 5G, the IoT, deep reinforcement learning, and software-defined networks.

VIET-THANG TRAN received the B.E. degree in electronic engineering from Can Tho University, Can Tho, Vietnam, in 1997, the M.S. degree in automatic engineering from Ho Chi Minh City University of Technology, Ho Chi Minh City, Vietnam, in 2003, and the Ph.D. degree in electronic engineering from Pukyong National University, Busan, South Korea, in 2016. Currently, he is with Vietnam Research Institute of Electronics, Informatics and Automation. His current research interests include ultra-low power sensor node design with energy harvesting, wireless sensor networks, IoT based application, and automation systems.

WAN-YOUNG CHUNG (Senior Member, IEEE) received the B.S. and M.S. degrees in electronic engineering from Kyungpook National University, Daegu, South Korea, in 1987 and 1989, respectively, and the Ph.D. degree in sensor engineering from Kyushu University, Fukuoka, Japan, in 1998. He was an Assistant Professor with Semyung University, from 1993 to 1999. He was an Associate Professor with Dongseo University, from 1999 to 2008. He has been a Full Professor with the Department of Electronic Engineering, Pukyong National University, South Korea, since 2008. His research interests include ubiquitous healthcare, wireless sensor network applications, and gas sensors.